



EUROPEAN ORGANIZATION FOR NUCLEAR RESEARCH

CERN/EP 82-213
23 December 1982

CORRELATION OF CHARM PARTICLES FROM GLUON-GLUON
FUSION IN HADRONIC COLLISIONS

S.N. Ganguli^(*) and M. Schouten
CERN, Geneva, Switzerland

ABSTRACT

In the framework of fusion process, $\sim 90\%$ of which is $g + g \rightarrow c + \bar{c}$, we have calculated rapidity correlation and p_T^2 of charm particles produced in hadronic collisions. The experimental observation of rapidity correlation by the LEBC-EHS Collaboration is in good agreement with the calculation. From the ratio of double to single charm production an estimate of fusion cross section is made.

Submitted to Nuclear Physics B

(*) On leave from Tata Institute of Fundamental Research, Bombay, India.

1. INTRODUCTION

There are two production mechanisms which are generally considered to be responsible for the associated production of charm states in hadronic interactions. These are, see fig. 1,

(a) fusion process

$$g + g \rightarrow c + \bar{c}, \quad q + \bar{q} \rightarrow c + \bar{c}, \quad (1)$$

and (b) flavour excitation process

$$g + c \rightarrow g + c, \quad q + c \rightarrow q + c, \quad \bar{q} + c \rightarrow \bar{q} + c. \quad (2)$$

These have been used extensively for the study of production cross sections and x distributions of charm hadrons, see for example refs [1-4]. The relative importance of the two mechanisms is still not clear. The reasons are the following: (a) the cross section depends strongly on the choice of M_c , the mass of the charm quark, and Λ , the strong coupling parameter, (b) the excitation process has additional problems due to poor knowledge of the charm structure function and the choice of \hat{t}_{\min} - the minimum momentum transfer of the gluon needed to excite a $c\bar{c}$ pair; it is also not clear whether the excitation process is distinct from the fusion one [1,4] and (c) the poor understanding of the recombination/fragmentation of the charm quark to form a D or Λ_c^+ hadron.

It is conceivable that the problem (c) mentioned above is minimal for the study of the correlation between the $D\bar{D}$ pair ($\Lambda_c^+\bar{D}$ is more complicated because of one extra quark in Λ_c^+ compared to D). The p_T^2 distribution of the charm quark is also expected to be nearly the same as that of $D/\bar{D}/\Lambda_c^+$ because of the massiveness of the charm quark. In this paper we would like to exploit the above argument to see how far one can understand the production of charm particles in the framework of the fusion process (without incorporating fragmentation/recombination) by comparing with the existing data. In sect. 2 we describe the details of the calculation. Numerical results and the comparison with the data are presented in sect. 3. In sect. 4 we have made an attempt to estimate the fusion cross section from the experimental data at $\sqrt{s} = 26$ GeV [5] and the summary in sect. 5.

2. DETAILS OF THE CALCULATION

The cross section for the production of a pair of charm quarks in a hadron-hadron collision is given by

$$\sigma_{c\bar{c}} = \int dx_1 \cdot dx_2 \cdot F_{1/A}(x_1, Q^2) \cdot F_{2/B}(x_2, Q^2) \cdot \frac{1}{x_1 x_2} \frac{d\hat{\sigma}}{d\hat{t}} d\hat{t} \quad (3)$$

where $\hat{\sigma}$ is the cross section for the subprocess $1 + 2 \rightarrow 3 + 4$ and the total cross section is obtained by summing over all the distinct subprocesses as given by (1) and (2); \hat{t} is the square of the 4-momentum transfer between partons 1 and 3. The structure functions $F_{1/A}$ and $F_{2/B}$ are the fractional momentum distributions of the partons inside the hadrons A and B; x_1 and x_2 are the momentum fractions carried by the partons 1 and 2 ($0 < x_{1,2} < 1$). In terms of the variables x_L and \hat{s} ,

$$\begin{aligned} x_L &= x_1 - x_2, \quad (-1 < x_L < +1) \\ \hat{s} &= s x_1 x_2 \end{aligned} \quad (4)$$

with x_L as the forward longitudinal momentum of the two partons 1 and 2, and \hat{s} as the subprocess energy in the fusion process, the eq. (3) can be rewritten as

$$\sigma_{c\bar{c}} = \int_{s_{th}}^s \int_{x_L=-1}^{+1} d\hat{s} \cdot dx_L \cdot F_{1/A} \cdot F_{2/B} \cdot \frac{1}{\hat{s}(x_1+x_2)} \cdot \frac{d\hat{\sigma}}{d\hat{t}} \cdot d\hat{t} \quad (5)$$

where s is the square of the c.m. energy of the initial hadrons A and B. The threshold value s_{th} of \hat{s} is taken as $4M_c^2$ with M_c as mass of the charm quark and the Q^2 has been taken [1] as $\hat{s}/2$ for $gg + c\bar{c}$ and \hat{s} for $q\bar{q} + c\bar{c}$. The Q^2 scale enters in the calculation through the structure functions and the QCD running coupling constant $\alpha(Q^2) = 12\pi/[25 \ln(Q^2/\Lambda^2)]$.

In the c.m. system of the initial hadrons A and B, we define $x_3 = 2p_3/\sqrt{s}$ and $x_4 = 2p_4/\sqrt{s}$ for the final charm pairs 3 and 4; the corresponding rapidities are y_3 and y_4 . The double differential cross sections for the fusion process are then given by (see Appendix for the derivations)

$$\frac{d^2\sigma}{dx_3 dx_4} = \int d\hat{s}. \frac{F_{1/A}(x_1, Q^2) \cdot F_{2/B}(x_2, Q^2)}{(x_L^2 + 4\hat{s}/s)} \cdot \frac{d\hat{\sigma}}{d\hat{t}} \quad (6)$$

$$\frac{d^2\sigma}{dy_3 dy_4} = \int dp_T^2 \cdot F_{1/A}(x_1, Q^2) \cdot F_{2/B}(x_2, Q^2) \cdot \frac{d\hat{\sigma}}{d\hat{t}} \quad (7)$$

where p_T^2 is the transverse momentum squared of the partons 3 and 4. The expressions for $d\hat{\sigma}/d\hat{t}$ are taken from ref. [1]. The variables x_L and \hat{s} are related to the kinematic variables of the outgoing charm quarks by the following expressions

$$\begin{aligned} x_L &= x_3 + x_4 \\ x_{3,4} &= 2 \cdot s^{-1/2} \cdot (M_c^2 + p_T^2)^{1/2} \cdot \sinh y_{3,4} \\ \hat{s} &= 2(M_c^2 + p_T^2)[1 + \cosh(y_3 - y_4)] \end{aligned} \quad (8)$$

From eqs (4) and (8) one can obtain the value of $x_{1,2}$ required for the structure functions in terms of $x_{3,4}$ (or $y_{3,4}$).

3. NUMERICAL RESULTS

The numerical calculations are carried out for the fusion process by using the following parametrizations of the structure functions:

- (a) Proton^(*); Valence quarks: parametrization of Buras and Gaemers [6], sea quarks: Owens and Reya [7] and gluons: from the neutrino data of the CDHS Collaboration [8].
- (b) Pion; We have used counting rule distributions for valence, sea and gluons corrected by the QCD Q^2 dependence [7].

(*) It may be mentioned that the total fractional momentum from these structure functions turns out to be 1.11. As the major contribution to the fusion process is due to the gluons ($\approx 90\%$) we have not made any attempt to normalise the total fractional momentum to unity.

The calculation of the cross section, as mentioned in sect. 1, depends strongly on the values of M_c and Λ ; in order to see the effects we have used for M_c values in the range 1.2 to 1.5 GeV and for Λ in the range 0.2 to 0.5 GeV (the variation in Λ matters only for the absolute value of the cross section).

3.1 Rapidity gap

No significant difference is found in the calculated rapidity gap, $\Delta y = |y_3 - y_4|$, distributions from πp and pp collisions. Figs 2(a)-2(c) show these distributions from pp collisions at $\sqrt{s} = 26$ and 62 GeV. Δy , Δy_{For} and $\Delta y_{\text{F-B}}$ in these distributions refer respectively to the overall rapidity gap, the rapidity gap with both the charm quarks in the forward hemisphere in the A-B c.m. system, and the rapidity gap with the two charm quarks in opposite hemispheres. The forward direction is taken to be the beam direction. The solid curves (with $M_c = 1.2$ GeV) and the dashed curves (with $M_c = 1.5$ GeV) are for $\sqrt{s} = 26$ GeV, and the dotted curves (with $M_c = 1.2$ GeV) are for $\sqrt{s} = 62$ GeV. It is seen from the figures that (a) the distributions are not sensitive to the choice of M_c in the range 1.2 to 1.5 GeV and (b) rapidity gap broadens with the increase of energy.

Table 1 summarises the average values of the rapidity gaps for the three above mentioned configurations of the $c\bar{c}$ pair; $\langle \Delta y \rangle$ as obtained here for πp (column 2) is in agreement with the calculation of ref. [9]. We have also listed in the table the fraction of events expected with both the charm quarks in the forward hemisphere.

The only result that exists for the rapidity gap is that of the LEBC-EHS Collaboration [5] at $\sqrt{s} = 26$ GeV. They have observed 5 $D\bar{D}$ pairs with both charm mesons in the forward hemisphere in the $\pi^+ p$ data and 1 in the pp data. The mean rapidity gap observed in the πp data from the 5 $D\bar{D}$ pairs is ≈ 0.5 which is in good agreement with our calculation of 0.56, see column 4 of table 1.

3.2 x and p_T^2 distribution

Figs 3(a) and 3(b) show the Feynman x distributions of the charm quark (with $M_c = 1.2$ GeV) in πp and pp collisions at $\sqrt{s} = 26$ GeV and are compared with the charm meson distributions as observed by the LEBC-EHS Collaboration. It is seen from the figures that the calculated x distributions (without incorporating hadronization of the charm quark to form D mesons) are not in good agreement with the data.

No significant difference is found between the calculated p_T^2 distribution of the charm quark in πp and pp collisions namely, the $\langle p_T^2 \rangle$ from πp and pp collisions at $\sqrt{s} = 26$ GeV are found to be 0.747 and 0.750 $(\text{GeV}/c)^2$ for the choice of $M_c = 1.2$ GeV. In fig. 4 we show the p_T^2 distributions for $\sqrt{s} = 26$ and 62 GeV with $M_c = 1.2$ GeV; for $p_T^2 \lesssim 3 (\text{GeV}/c)^2$ the distributions are reasonably exponential. The calculated values of $\langle p_T^2 \rangle$ for the choice of M_c in the range 1.2 to 1.5 GeV are,

$$\langle p_T^2 \rangle = 0.75 - 1.0 (\text{GeV}/c)^2 \quad \text{at } \sqrt{s} = 26 \text{ GeV,}$$

$$\langle p_T^2 \rangle = 1.0 - 1.4 (\text{GeV}/c)^2 \quad \text{at } \sqrt{s} = 62 \text{ GeV.}$$

These values are in reasonable agreement with the experimental data of D/\bar{D} production which give $\langle p_T^2 \rangle = 0.9 \pm 0.2 (\text{GeV}/c)^2$ at $\sqrt{s} = 26$ GeV [5] and $\langle p_T \rangle \sim 0.9$ GeV/c at $\sqrt{s} = 62$ GeV [10].

4. ESTIMATION OF FUSION CROSS SECTION

In the previous section we have seen that the rapidity gap and p_T^2 distribution of the experimentally observed charm mesons can be explained in terms of the fusion process. The next obvious point is to estimate the fusion cross section. This can be deduced from the experimental ratio of double to single charm production in the forward hemisphere. The expected ratio from the fusion process (column 6 of table 1) is 0.6 to 0.7 at $\sqrt{s} = 26$ GeV. The last column of table 1 gives the experimental data at $\sqrt{s} = 26$ GeV. Clearly this number is a lower estimate because (a) more topological pairs are seen [5] but they cannot be reconstructed because more than one decay particles are outside the spectrometer acceptance, and (b) $\Lambda_c^+ \bar{D}$ pairs are not seen probably

because Λ_c^+ has too short a lifetime ($\sim 10^{-13}$ s) to be distinctly visible in LEBC; this also explains why one sees less pairs in pp collisions compared to πp . We therefore estimate a lower limit on the contribution of the fusion process in πp collisions (with the assumption^(*) that the charm pairs in the forward hemisphere are all due to this process) and it is $\gtrsim 70\%$, i.e. the total fusion cross section is $\gtrsim 30 \mu\text{b}$ at $\sqrt{s} = 26$ GeV. A note of caution: the result is based on poor statistics.

We now evaluate the fusion cross section by making numerical integration of eq. (3). Because of the dominance of the gluon-gluon fusion ($\sim 90\%$) the results from πp and pp collisions are essentially the same within 10%. The numerical results are therefore presented in table 2 for pp collisions at $\sqrt{s} = 26$ and 62 GeV. For the sake of completeness we have also presented the cross sections from the excitation process based on the prescription of ref. [1] with charm structure function of ref. [6] and with $\hat{s} = M_c^2 + s x_1 x_2$; for the excitation process $\hat{t}_{\min} = 2M_c^2$ is preferred [11]. The effects on the cross section due to variation in the values of M_c , Λ and \hat{t}_{\min} are clearly seen from the table. It is interesting to note that one could get charm production cross section of 38 and 140 μb - with $M_c = 1.2$ GeV and $\Lambda = 0.5$ GeV - from fusion process at $\sqrt{s} = 26$ and 62 GeV respectively, which are not too low.

5. SUMMARY

In this paper we have made an attempt to see to what extent the fusion process can explain charm production in hadronic collisions. We have not incorporated recombination/fragmentation of the charm quark; this could be the reason for obtaining a steeper x distribution than the experimental data. As regards rapidity gap and p_T^2 distributions we believe that this effect is minimal. Indeed we find that our calculated values are in good agreement with the existing data. We have also made an estimate of

(*) It may be noted that in the excitation process according to the QCD Monte-Carlo calculation of Odorico [3] the struck and the spectator charm quark fall in opposite hemisphere at these energies.

the fusion cross section as $\gtrsim 30 \mu\text{b}$ at $\sqrt{s} = 26 \text{ GeV}$ by comparing the experimental ratio of double to single charm production in the forward hemisphere with the calculated one, but much better experimental data are needed before a firm conclusion can be drawn. The expected value of the fusion cross section at this energy is $38 \mu\text{b}$ with the choice of M_c as 1.2 GeV and Λ as 0.5 GeV .

Acknowledgements

One of us (S.N.G.) would like to thank Drs L. Montanet and S. Reucroft for the warm hospitality given to him in the CERN EHS group.

APPENDIX

Derivation of the double differential distributions in terms of x , y and p_T^2 for $c\bar{c}$ in fusion process:

In the fusion process $1 + 2 \rightarrow 3 + 4$, where 3 and 4 are the $c\bar{c}$ pair and 1 and 2 are the massless colliding partons with the +ve z axis along the parton 1, the square of the 4 momentum transfer between 1 and 3 can be written in the 1-2 c.m. system as,

$$\begin{aligned} \hat{t} &= M_c^2 - 2E_1^* E_3^* + 2 P_{1\parallel}^* P_{3\parallel}^* \\ &= M_c^2 - \hat{s}/2 + \sqrt{\hat{s}} \cdot P_{3\parallel}^* \end{aligned} \quad (A1)$$

where \hat{s} is the square of the c.m. energy of the 1-2 system and M_c the mass of the c quark. We neglect transverse momentum of the colliding partons. We now express $P_{3\parallel}^*$ in terms of variables defined in the c.m. system of the initial hadrons A and B using the Lorentz factors,

$$\begin{aligned} \bar{\gamma} &= (x_1 + x_2) \cdot (s/4\hat{s})^{1/2}, \\ \bar{\gamma}\bar{\beta} &= (x_1 - x_2) (s/4\hat{s})^{1/2} \end{aligned} \quad (A2)$$

where x_1 and x_2 are the momentum fractions carried by the partons 1 and 2 in the A-B c.m. system and s is c.m. energy square of the A-B system

$$\begin{aligned} P_{3\parallel}^* &= \bar{\gamma} (P_{3\parallel} - \bar{\gamma}\bar{\beta} E_3^*) / (1 + \bar{\gamma}^2 \bar{\beta}^2) \\ &= \frac{1}{2} \bar{\gamma} (\sqrt{s} x_3 - \bar{\gamma}\bar{\beta} \sqrt{\hat{s}}) / (1 + \bar{\gamma}^2 \bar{\beta}^2) \end{aligned} \quad (A3)$$

where x_3 is the Feynman x value of the charm quark 3. Substituting the above expression in (A1) we get

$$\hat{t} = M_c^2 + s \cdot (x_3 - x_1) \cdot \frac{x_1 x_2}{(x_1 + x_2)} \quad (A4)$$

which is in agreement with that of ref. [2].

Now using (A4) and eq. (5) of sect. 2 we have the following form for the double differential distribution

$$\frac{d^2\sigma}{dx_3 dx_L} = \int d\hat{s} \cdot \frac{F_{1/A} \cdot F_{2/B}}{(x_1 + x_2)^2} \cdot \frac{d\hat{\sigma}}{d\hat{t}}$$

since $x_L = x_3 + x_4$, where we define x_4 as the Feynman x for the charm quark 4 in the A-B c.m. system, we get

$$\frac{d^2\sigma}{dx_3 dx_4} = \int d\hat{s} \cdot \frac{F_{1/A} \cdot F_{2/B}}{(x_1 + x_2)^2} \cdot \frac{d\hat{\sigma}}{d\hat{t}} \quad (A5)$$

Similarly, using the relations

$$x_{3,4} = 2 \cdot s^{-1/2} \cdot \hat{M} \sinh y_{3,4}$$

$$\hat{M} = (M_C^2 + p_T^2)^{1/2}$$

we obtain the following form for x_L

$$x_L = 2 s^{-1/2} \cdot \hat{M} (\sinh y_3 + \sinh y_4)$$

The differential distribution in terms of y_3 and y_4 is then given by

$$\frac{d^2\sigma}{dy_3 \cdot dy_4} = \int d\hat{s} \cdot \frac{F_{1/A} \cdot F_{2/B}}{s(x_1 + x_2)^2} \cdot 4\hat{M}^2 \cdot \cosh y_3 \cdot \cosh y_4 \cdot \frac{d\hat{\sigma}}{d\hat{t}} \quad (A6)$$

Eq. (8) of sect. 2 yields

$$\frac{d\hat{s}}{dp_T^2} = \frac{(\cosh y_3 + \cosh y_4)^2}{\cosh y_3 \cdot \cosh y_4}$$

substituting this in eq. (A6) we have the form

$$\frac{d^2\sigma}{dy_3 \cdot dy_4} = \int dp_T^2 \cdot F_{1/A} \cdot F_{2/B} \cdot \frac{d\hat{\sigma}}{d\hat{t}} \quad (A7)$$

which is in agreement with ref. [4]. The p_T^2 distribution can be obtained from this by integrating over y_3 and y_4 .

REFERENCES

- [1] B.L. Combridge, Nucl. Phys. B151 (1979) 429.
- [2] V. Barger, F. Halzen and W.Y. Keung, Phys. Rev. D25 (1982) 112.
- [3] R. Odorico, Bologna preprint IFUB 82/3.
- [4] R. Winder and C. Michael, Nucl. Phys. B173 (1980) 59.
- [5] LEBC-EHS Collaboration, M. Aguilar-Benitez et al., preprints CERN/EP 82-203, CERN/EP 82-204.
- [6] A.J. Buras and K.J.F. Gaemers, Nucl. Phys. B132 (1978) 249.
- [7] J.F. Owens and E. Reya, Phys. Rev. D17 (1978) 3003.
- [8] CDHS Collaboration, H. Abramowicz et al., Zeitsch. für Phys. C12 (1982) 289.
- [9] R.J.N. Phillips, Proc. of Moriond Workshop on New Flavours, p. 467 (1982), edited by J. Tran Than Van and L. Montanet.
- [10] M. Basile et al., Lett. Nuovo Cim. 33 (1982) 17.
- [11] B.J. Edwards and T.D. Gottschalk, Nucl. Phys. B196 (1982) 328.

TABLE 1

Correlation of charm particles(*)

\sqrt{s} (GeV)	$\langle \Delta y \rangle$	$\langle \Delta y \rangle_{F-B}$ one forward and the other backward	$\langle \Delta y \rangle_{For}$ both forward	fraction of cc with both in forward hemisphere	Ratio of double to single charm in forward hemisphere	
					Theory	Expt. data
26 ($\pi^- p$)	0.83	1.21	0.56	0.30	0.7	5/10 [5]
26 (pp)	0.83	1.20	0.53	0.28	0.6	1/19 [5]
62 (pp)	1.0	1.52	0.72	0.31	0.8	-

(*) Calculated values are averaged over $M_c = 1.2$ and 1.5 GeV.

TABLE 2

Charm production cross section in pp collisions

(a) Effect of M_c (with $\Lambda = 0.5$ GeV, $\hat{t}_{\min} = 2 M_c^2$)

\sqrt{s} (GeV)	M_c (GeV)	Fusion (μb)	Excitation (μb)
26	1.2	38	34
	1.3	25	22
	1.5	11	10
62	1.2	140	244
	1.3	100	177
	1.5	55	97

(b) Effect of Λ (with $M_c = 1.2$ GeV, $\hat{t}_{\min} = 2 M_c^2$)

\sqrt{s} (GeV)	Λ (GeV)	Fusion (μb)	Excitation (μb)
26	0.2	15	9
	0.3	21	15
	0.5	38	34
62	0.2	57	64
	0.3	80	107
	0.5	140	244

(c) Effect of \hat{t}_{\min} (with $M_c = 1.2$ GeV, $\Lambda = 0.5$ GeV)

\sqrt{s} (GeV)	\hat{t}_{\min}	Fusion (μb)	Excitation (μb)
26	M_c^2	38	126
	$1.5 M_c^2$	38	63
	$2 M_c^2$	38	34
62	M_c^2	140	733
	$1.5 M_c^2$	140	399
	$2 M_c^2$	140	244

FIGURE CAPTIONS

- Fig. 1 Schematic diagrams for charm production from (a) fusion process:
 $g + g \rightarrow c + \bar{c}$ and $q + \bar{q} \rightarrow c + \bar{c}$, and (b) excitation process:
 $g + c \rightarrow g + c$ and $q + c \rightarrow q + c$.
- Fig. 2 Rapidity gap distributions of charm pairs from $pp \rightarrow c\bar{c} + X$, (a) all charm quark pairs, (b) both charm quarks in the forward hemisphere and (c) charm quarks in opposite hemispheres. The solid curves (with $M_c = 1.2$ GeV) and the dashed curves (with $M_c = 1.5$ GeV) are for $\sqrt{s} = 26$ GeV; and the dotted curves (with $M_c = 1.2$ GeV) are for $\sqrt{s} = 62$ GeV.
- Fig. 3 Feynman x distributions of charm for (a) πp interactions and (b) pp interactions at $\sqrt{s} = 26$ GeV. The curves present the calculations as described in the text, with $M_c = 1.2$ GeV and $\Lambda = 0.5$ GeV. The histograms are experimental data from ref. [5]. The curves are normalized to the same total number of events as the data.
- Fig. 4 p_T^2 distributions of charm quarks at $\sqrt{s} = 26$ GeV and 62 GeV.

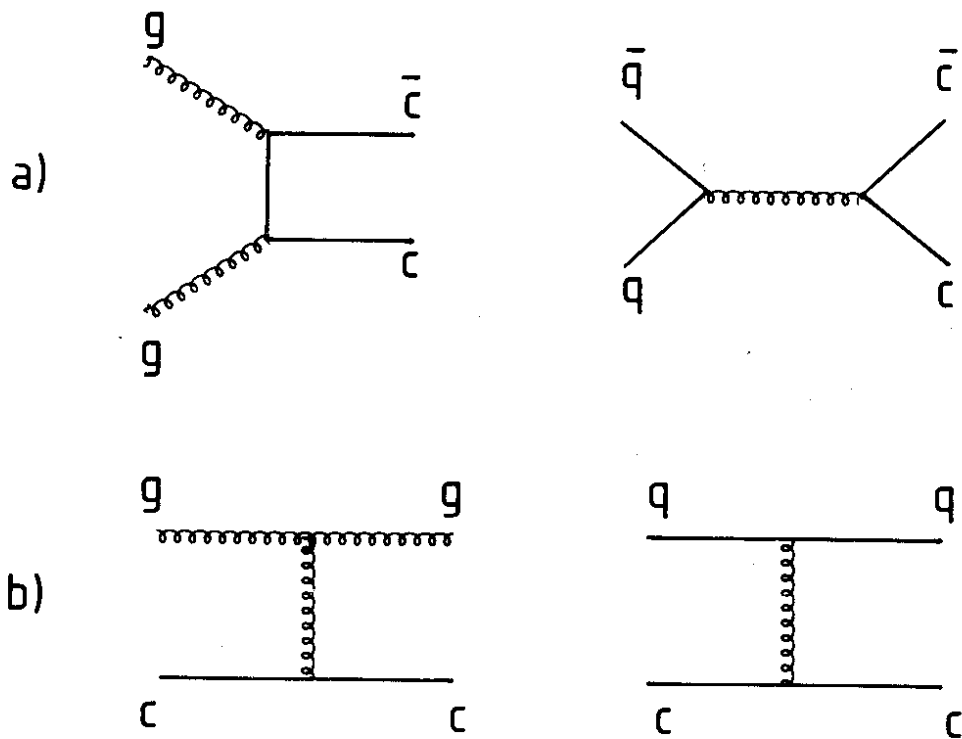


Fig. 1

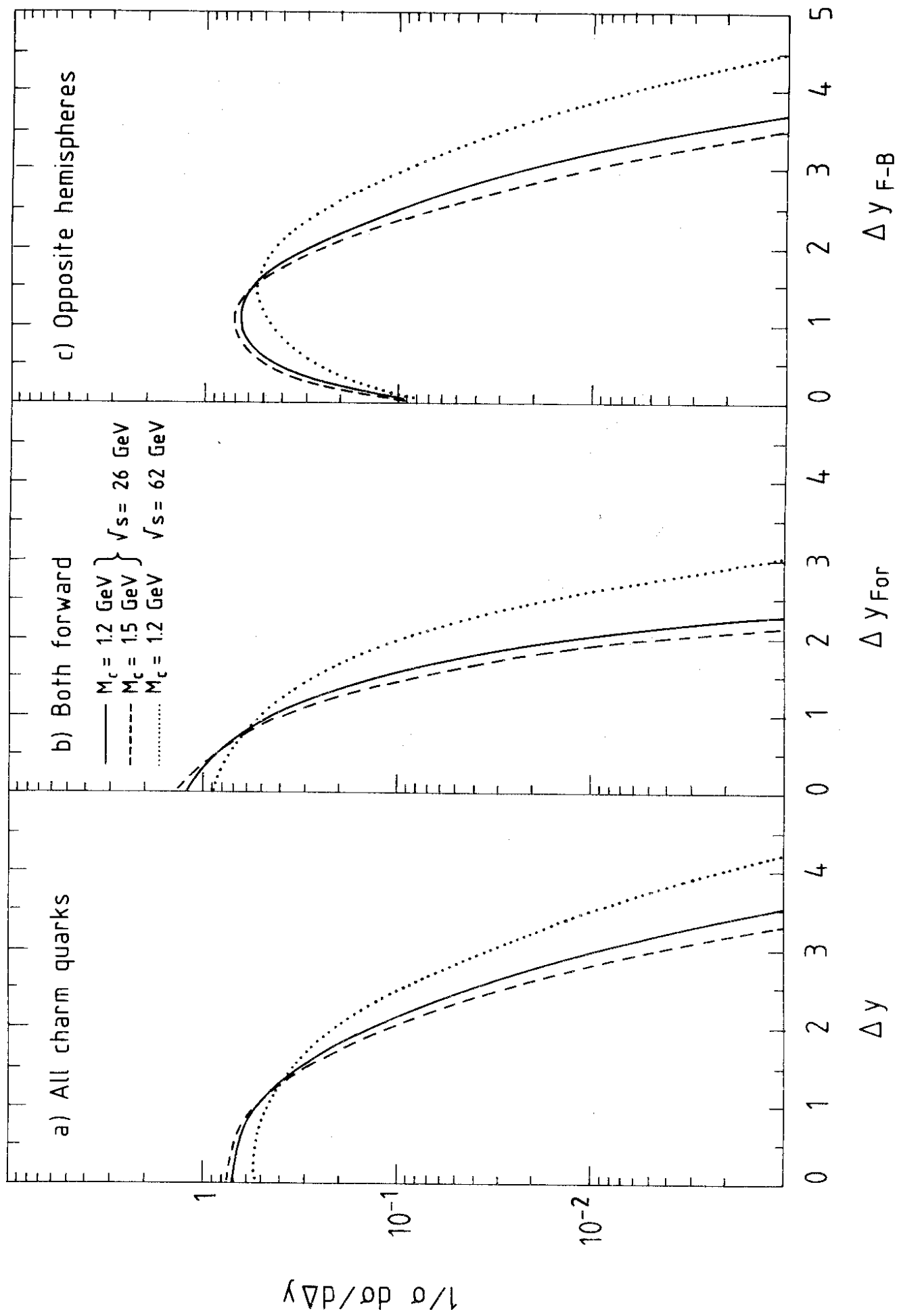


Fig. 2

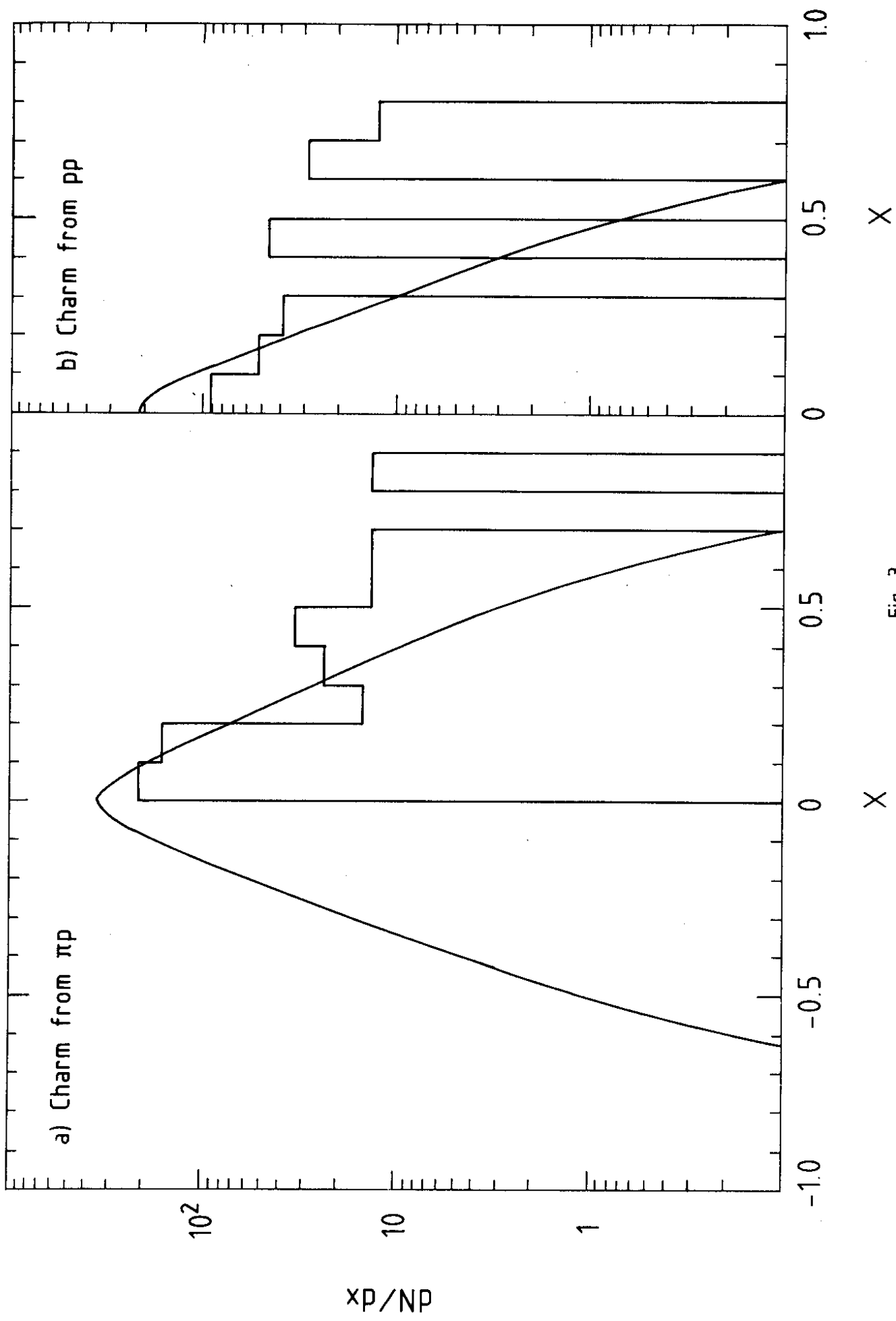


Fig. 3

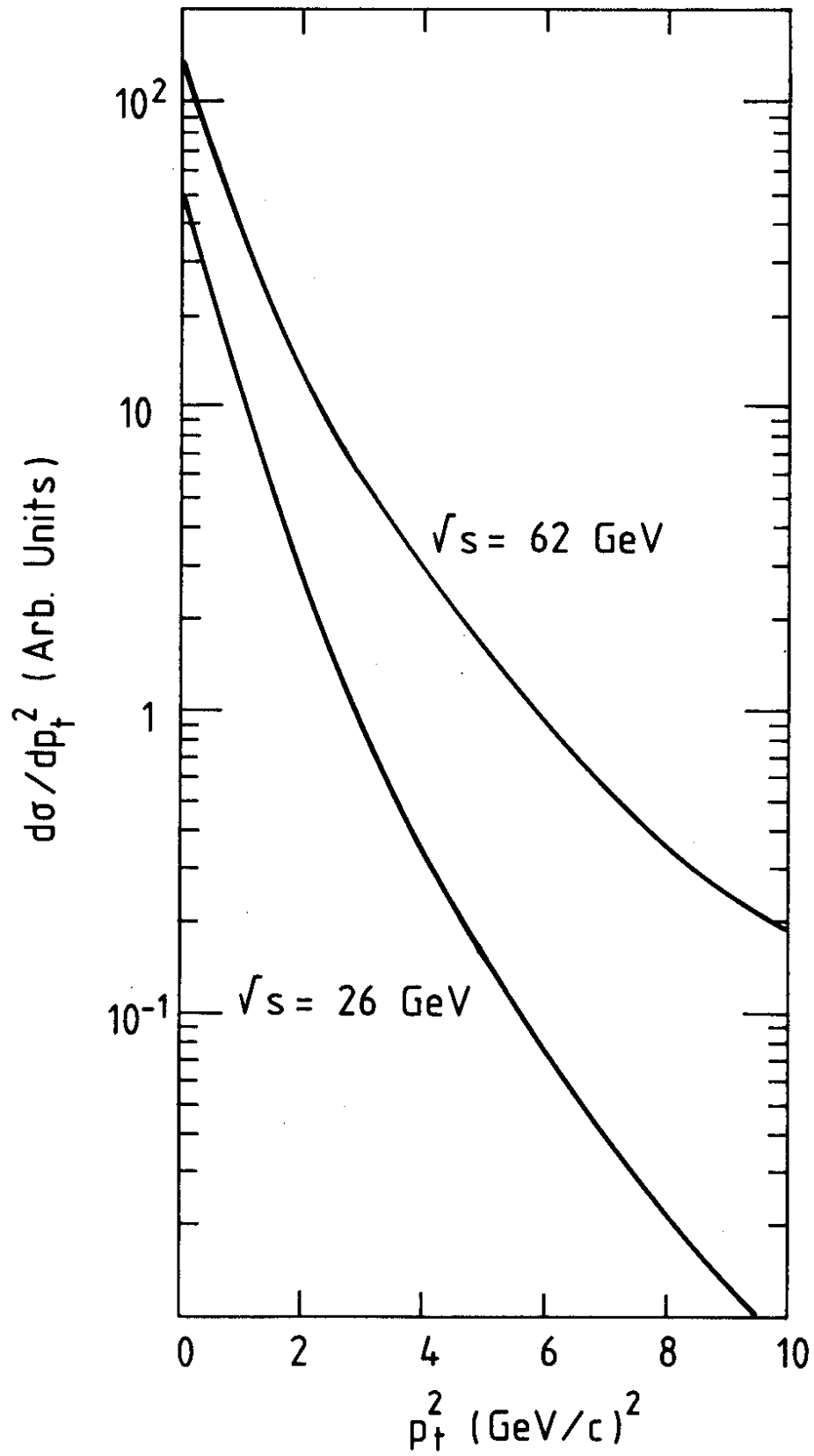


Fig. 4